Adsorption (2013) 19:91–99
DOI 10.1007/s10450-012-9422-2

Adsorption of methyl parathion on PAC from natural waters: the effect of NOM on adsorption capacity and kinetics

Jingyi Zhang · Baoyou Shi · Tao Li · Dongsheng Wang

Received: 30 December 2011 / Accepted: 14 September 2012 / Published online: 29 September 2012

Abstract Source water pollution by agricultural chemicals poses great threat to drinking water safety and the removal of such contaminants is a challenge to the water treatment industry. In this work, the adsorption behaviors of methyl parathion (MP) from different natural waters onto different kinds of powdered activated carbons (PAC) were investigated systematically. On the basis of the characterization of the PACs and natural organic matter (NOM), the suitability of PAC with NOM for effective removal of MP was proposed, and the effect of competitive adsorption on MP removal under two PAC dosing patterns was evaluated. The results indicated that NOM adsorption was dependent on the molecular weight (MW) distribution of organic compounds and the pore size distribution of PAC. The mesopore surface area with pore size > 3 nm was dominant for the adsorption of the NOM fraction in the range of 500 Da $<$ MW $<$ 3000 Da. Competition for adsorption sites by smaller MW NOM had significant effect on the adsorption of target organic compound in the simultaneous adsorption pattern. Whereas in the NOM-preloaded adsorption pattern, pore blockage by relatively larger MW NOM resulted in markedly reduction in both adsorption capacity and adsorption kinetics, the diffusion rate of MP on PAC could be affected by the PAC dosage, pore size distribution and the MW distribution of NOM.

Keywords Powdered activated carbon (PAC) · Natural organic matter (NOM) · Suitability · Competitive adsorption · Pore blockage

J. Zhang · B. Shi (✉) · T. Li · D. Wang
State Key Laboratory of Environmental Aquatic Chemistry, Research Center for Eco-Environmental Sciences, Chinese Academy of Sciences, Beijing 100085, China
e-mail: byshi@rcees.ac.cn

1 Introduction

With the enhancement of human activities and large-scale use of agricultural chemicals, synthetic organic pollutants have been detected in natural waters worldwide, and even water pollution accidents by organic chemicals are frequently reported. Water pollution events not only result in the deterioration of water quality, severely affecting the water ecological environment, but also have adverse impacts on economic and social activities (Zhang et al. 2011). Source water pollution by accidental events and misconduct discharge of industrial waste are great threat to drinking water safety and security. Emergency control and management systems for water pollution are necessary to help water industries duly make decisions and respond effectively (He et al. 2011).

Activated carbon adsorption is one of the most often used technologies for the removal of natural or synthetic organic compounds in water. The United States Environmental Protection Agency regarded activated carbon adsorption as the best available technology for the removal of organic contaminants limited in the environmental regulations. Powered activated carbon (PAC) adsorption is among the preferred emergency treatment technologies for source water pollution events because of its operational convenience and efficiency (Abou-Mesalam 2003; Shin and Rowell 2005; McKay and Choy 2005). Compared with other technologies, the PAC adsorption process can be easily operated and induces minimal secondary pollution. However, widely acceptable guidelines for PAC application in emergency treatment are not yet established because of insufficient knowledge of the factors affecting PAC treatment efficiency.

Natural organic matter (NOM) in water can adversely affect the adsorption of trace organic pollutants (Carter and

Weber 1994; Kilduff et al. 1998) by activated carbons, and the two primary mechanisms involved are believed to be direct surface site competition and blockage of activated carbon pores by NOM (Carter and Weber 1994; Li et al. 2003b, 2003c). A competitive adsorption model for flow-through PAC systems was developed by Li et al. using p-dichlorobenzene and poly(styrene sulfonate) as NOM surrogates (Li et al. 2003a), and the model was verified by Ding et al. using natural ground waters (Ding et al. 2006). NOM adsorption was also found to correlate well with the surface area of activated carbon pores in the diameter range of 15–50 Å (Ding et al. 2006). However, the molecular structure and composition of NOM are rather complicated and vary depending on geological and vegetation characteristics. NOM from different sources have different physical and chemical fractionation features (Wei et al. 2008), which could exhibit different adsorption behaviors on activated carbon, and the effect of different NOM sources and fractions on the adsorption of synthetic organic pollutants require further elucidation. Moreover, the suitability between NOM fractionation characteristics and activated carbon characteristics is still not fully understood.

Organic agricultural chemicals are common type of contaminants in the event of pollution of source waters. Methyl parathion (MP), a typical organic phosphorus pesticide, has been widely used in the past years because of its low cost and high efficiency against many pests in various crops (Li et al. 2011; Akhtar et al. 2009; De Souza and Machado 2006). MP can act as an acetyl cholinesterase inhibitor in human body, disturbing the function of the nervous system (Gogate and Shriwas 2011). The extensive use of organic phosphorous pesticides for pest control has raised serious public concern regarding health, environment, and food safety because of the high toxicity of such chemicals (Arduini et al. 2006; Li et al. 2007).

In this work, raw surface waters with different NOM characteristics were collected as test waters, and MP was used as the target synthetic organic pollutant. A series of batch isotherm and kinetic experiments were performed using PACs with different pore size distributions (PSD). The relationship between the PSD of PAC and the molecular weight distribution (MWD) of NOM was quantitatively evaluated using high performance size exclusion chromatography (HPSEC). Furthermore, the effect of two different dosing patterns in the emergency treatment of pollution events was assessed, and the possible mechanism involved was discussed. Results obtained in the present work could provide instructive reference for the emergency treatment of drinking source water pollution.

2 Materials and methods

2.1 Materials

2.1.1 Water

Organic-free water (OFW) was obtained by passing deionized water through a NANO ultrapure water system. The dissolved organic carbon (DOC) concentration of the organic-free water was less than 0.03 mg/L. OFW was buffered with 10^{-3} M Na_2CO_3, and the pH was adjusted to 7.8 using sodium hydroxide for control adsorption experiments. Natural waters were collected from two reservoirs at a distance far from each other, MiYun reservoir (denoted as MY) in Beijing, China and MoPanShan reservoir (denoted as MPS) in Harbin, northeast of China. The raw waters were stored at 4 °C after collection. Prior to use, the water was warmed up to ambient temperature and filtered through a 0.45 μm membrane filter to remove suspended solids.

2.1.2 Adsorbent

Three PACs with different PSDs were used in the present work, namely, PAC1, PAC2, and PAC3. PAC1 and PAC2 were two commercial activated carbons made from coal and fruit shell, respectively. PAC3 was prepared in the laboratory using coconut shell by chemical activation ($ZnCl_2$ as activation agent). All PACs were stored in desiccators for later use.

The surface area and PSD parameters were determined by the N_2 adsorption isotherm technique using Quadrasorb SI Surface Area and Pore Size Analyzer (Quantachrome, USA).

2.1.3 Adsorbate

Methyl parathion (MP) was purchased from J&K Scientific Ltd. The molecular formula of MP is $C_8H_{10}NO_5PS$ with IUPAC chemical name *O*,*O*-dimethyl *O*-4-nitrophenyl-phosphorothioate. The molecular weight of MP is 263.5, melting point 37.5 °C, Log octanol–water partition coefficient 3.00 (Schwarzenbach et al. 2003). A stock solution of MP in methanol was used to prepare all test solutions. The concentration of MP was measured using high performance liquid chromatography (HPLC, Waters 1525, USA).

2.2 Adsorption isotherm experiments

2.2.1 Isotherm tests using fresh PACs

Different amounts of fresh PACs were added into 40 mL-vials with certain concentration of MP solution prepared by OFW, natural waters (MY or MPS), respectively. The vials

were placed in a thermostatic mechanical shaker with a frequency of 200 rad/min for 24 h at 25 °C (previous tests proved that 24 h was sufficient to reach adsorption equilibrium). Adsorption systems were filtered through a 0.45 µm membrane to remove carbon, and the residual MP concentration of the filtrate was analyzed using HPLC. Vials without carbon additions were included in each batch as control to determine any possible MP loss, except for PAC adsorption. The Freundlich model was used to fit the adsorption isotherms.

$$q = K C_{eq}^{1/n}$$

where q and C_{eq} are equilibrium concentrations of the adsorbent in the solid (mg/g) and liquid phases (mg/L), respectively. K and $1/n$ are Freundlich constants.

2.2.2 Isotherm tests using NOM preloaded PACs

To mimic the PAC dosing pattern in front of the pollution spot, fresh PACs were preloaded with NOM by adding them into raw natural waters for 3 days. After preloading, different amount of MP stock solutions were spiked into the vials containing the preloaded PACs to obtain test suspensions with different MP concentrations. The vials were shaken for an additional 24 h for MP adsorption.

2.3 Adsorption kinetic experiments

MP adsorption kinetic experiments were conducted in three ways, namely, in OFW with fresh PACs, in natural waters with fresh PACs, and in natural waters with preloaded PACs. Operation procedures similar to those in the previous adsorption isotherm tests were followed. Samples were taken at different time intervals for residual MP concentration measurement. The homogeneous surface diffusion model (HSDM) was used to fit the kinetic data (Hand et al. 1983; Hung et al. 2005).

2.4 PSD Analysis

PSD analysis was performed using N_2 gas adsorption at 77 K with an Autosorb^{-1} Volumetric Sorption Analyzer controlled by Autosorb^{-1} software (Quantachrome). All samples were degassed at 150 °C until the outgas pressure rise was below 5 µmHg/min prior to analysis. The Brunnauer–Emmett–Teller (BET) surface area was determined from the N_2 adsorption isotherm. The total pore volume was estimated from the amount of nitrogen adsorbed at the relative partial pressure $P/P_0 = 0.95$. The t-method was applied to determine the PSD and pore volume information.

2.5 MWD analysis of NOM

The MWD of NOM was obtained using the HPSEC method. The instrument was HPLC (Waters 1525, USA) with gel chromatography column (Shodex Protein KW-802.5, Sholo, Japan). The flow rate of the mobile phase was 0.8 mL/min, which comprised 0.02 M orthophosphate at pH 6.8. NaCl was added to yield an ionic strength of 0.1 M. Prior to use, the mobile phase was degassed for at least 1 h to prevent air bubbles from entering the SEC column. The calibration curve was generated using polystyrene sulfonate (PSS) with molecular weight (MW) ranging from 1800 Da to 35,000 Da and acetone (MW = 58 Da). The UV absorbance of PSS and acetone was monitored at 224 nm. When NOM was analyzed, a 20 mL sample was taken and filtered through a 0.22 µm membrane filter. The first 10 mL were discarded to eliminate error attributable to the adsorption of NOM on the membrane and the leaching of organics from the membrane, and the remaining 10 mL were transferred into a sample vial for HPSEC analysis. The UV absorbance of the sample was monitored at 254 nm.

3 Results and discussion

3.1 PSD Characteristics of PACs and MWD characteristics of NOM

3.1.1 PSD characteristics of PACs

Table 1 provides the physical characteristics of three PACs. Among the three PACs, PAC3 had the highest BET surface area, micropore and mesopore surface areas, as well as the highest total pore volume and micropore volume. However, the mesopore volume of PAC3 was less than that of PAC2, and the average pore diameter of PAC3 was the smallest. PAC2 had the highest mesopore volume and all other parameters were between PAC1 and PAC3. PAC1 had the largest average pore diameter, but all other parameters were the smallest among the three PACs. The BET surface area, micropore and mesopore surface areas, and the total

Table 1 Characteristics of the three PACs

	PAC1	PAC2	PAC3
BET surface area (m^2/g)	807	1162	1493
Micropore surface area (m^2/g)	780	1037	1331
Mesopore surface area (m^2/g)	26.8	125.4	162.3
Total pore volume (cm^3/g)	0.552	0.683	0.779
Micropore volume (cm^3/g)	0.490	0.500	0.622
Mesopore volume (cm^3/g)	0.062	0.183	0.158
Average pore diameter (nm)	2.737	2.350	2.088

pore and micropore volumes of three PACs follow the order: PAC3 > PAC2 > PAC1. On the other hand, mesopore volume follows the order: PAC2 > PAC3 > PAC1. The average pore diameter follows the order: PAC1 > PAC2 > PAC3.

Figure 1 shows the mesopore size distributions of three PACs. Although the mesopore surface area and total pore volume of PAC3 were both higher than those of PAC1, the mesopore amount of PAC3 with pore size > 3 nm was less than that of PAC1. By contrast, the mesopore surface area and volume of PAC2 were higher than those of PAC1, and the mesopore amount of PAC2 exceeded that of PAC1 within the mesopore size range.

3.1.2 MWD characteristics of NOM

Table 2 presents the NOM characteristics of two raw waters, MY and MPS. HPSEC and resin fractionation (Wei et al. 2008) methods were used to characterize the constituents of NOM. The NOM concentration of MPS water was nearly thrice that of MY water. The NOM of MY water had a significantly higher hydrophilic fraction and slightly lower fraction with molecular weight in the range of 500 Da < MW < 3000 Da. The hydrophobic NOM fraction with MW greater than 1000 Da can be easily adsorbed by PAC because this fraction is more likely to access the hydrophobic surface of PAC.

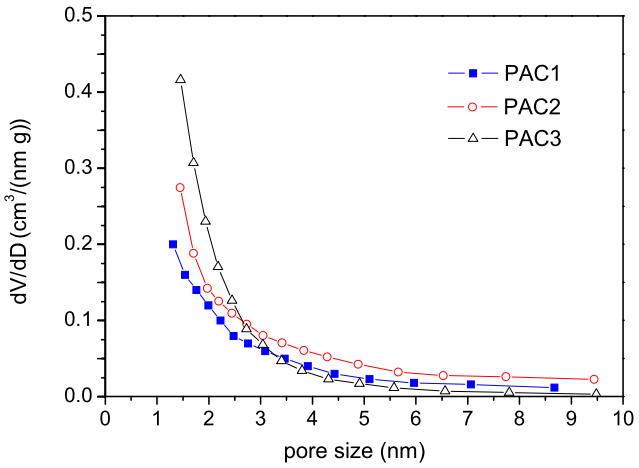

Fig. 1 Mesopore size distribution of PAC1, PAC2, and PAC3 based on the BJH model

3.2 Suitability of the PSD of PACs with the MWD of NOM

To investigate the effect of PSD of PAC on NOM adsorption, PAC1 and PAC3 were selected for comparative study because of their significantly different mesopore size distribution. The tests were conducted using MY water samples, and the water samples after adsorption by two PACs were analyzed using HPSEC. Figure 2 shows the apparent molecular weight (AMW) of NOM before and after adsorption by different dosages of the two PACs. With 2 and 4 mg/L PAC dosages, NOM with MW < 500 Da was primarily removed, whereas the adsorption of NOM with MW > 500 Da was insignificant.

The surface areas of PACs were primarily comprised of micropores (Table 1). Micropores can be easily accessible for smaller NOM. Figure 2 shows that only the NOM fraction with low MW was adsorbed at low carbon doses. By contrast, the NOM fraction with high MW was rarely adsorbed because the surface area accessible for this fraction was limited at low PAC doses. With the increase in carbon dose, the adsorbed amount of NOM with 500 Da < AMW < 3000 Da increased. The smaller and larger molecular NOM fractions were demonstrated to be adsorbed on different surface sites. NOM with AMW < 500 Da was primarily adsorbed in the micropores, whereas that with 500 Da < AMW < 3000 Da was primarily adsorbed in the mesopores. This observation agrees with the findings of Li et al. (2003b).

A comparison between Figs. 2a and 2b reveals that the peaks of PAC3 at AMW < 300 Da are lower than those of PAC1, and the peaks of PAC3 at 500 Da < AMW < 1200 Da are higher than those of PAC1. These phenomena indicated that the adsorption capacity of PAC3 was stronger than that of PAC1 for lower AMW NOM, whereas weaker for higher AMW NOM. This finding could be explained in terms of the differences in the PSD of the two PACs and the MWD of NOM. The high adsorption capacity of PAC3 for lower MW NOM was primarily attributable to its relatively higher micropore area and micropore volume (Table 1).

Although the mesopore area of PAC3 was also higher than that of PAC1, the adsorption capacity of PAC3 for larger MW NOM was not. The specific mesopore size distribution of the two PACs should be introduced to explain this phenomenon. The mesopore surface area and volume of PAC3 were both higher than those of PAC1 (Table 1). However, the mesopore surface area and volume of

Table 2 NOM characteristics of raw waters from the MY and MPS reservoirs

Water sample	DOC mg/L	Physical fraction (%) 500 Da < MW < 3000 Da	Chemical fraction (%)	
			Hydrophilic	Hydrophobic
MY	2.0	70	42	58
MPS	5.8	85	20	80

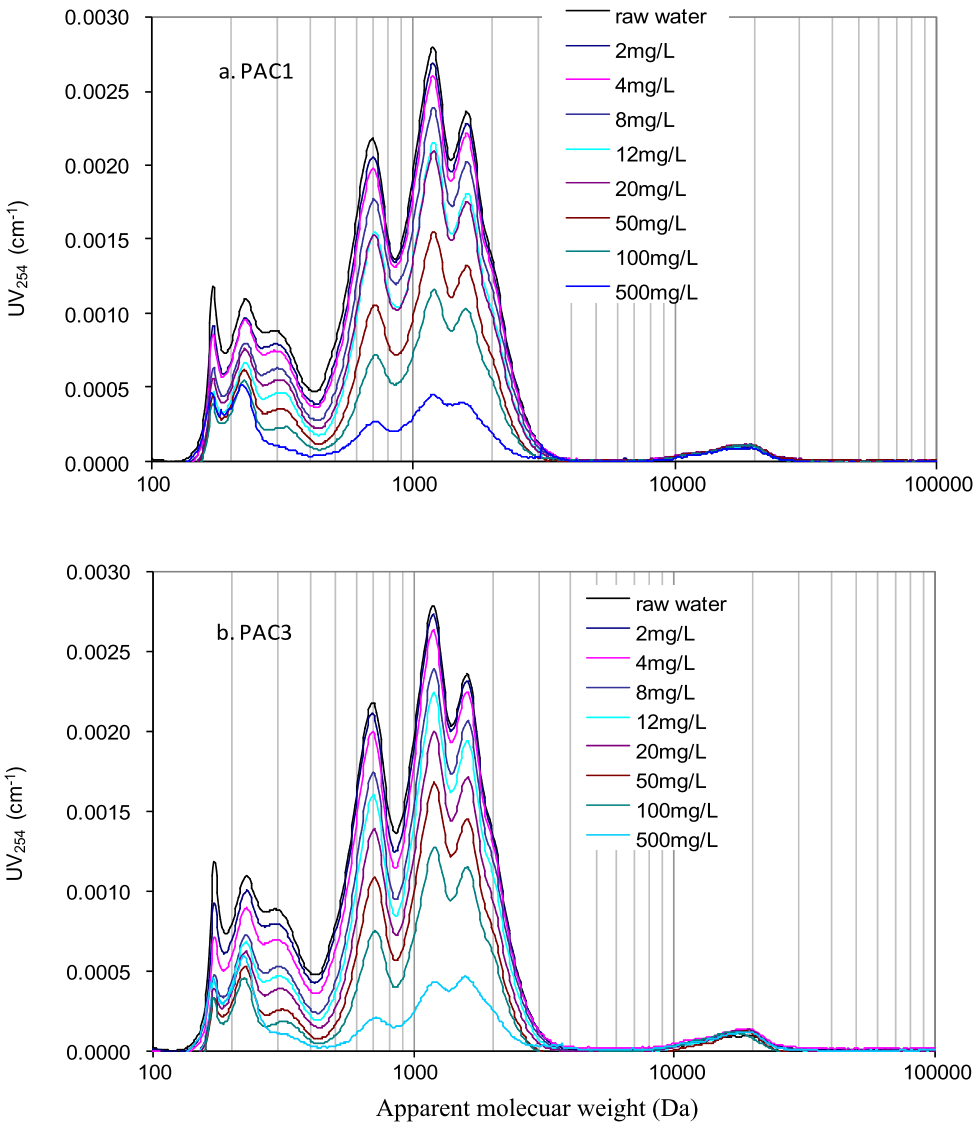

Fig. 2 AMW distribution of NOM for MY reservoir water before and after adsorption at different PAC dosages (**a** PAC1; **b** PAC3)

PAC3 primarily comprised of mesopores with diameter < 3 nm (Fig. 1). The mesopore amount of PAC3 with pore size > 3 nm was less than that of PAC1. Therefore, it could be inferred that the relatively larger MW NOM fractions (500 Da < AMW < 1200 Da) were primarily adsorbed by mesopores with pore size > 3 nm. The stronger adsorption capacity of PAC1 for larger MW NOM was attributable to its higher mesopore amount with pore size > 3 nm. Although PAC3 contained more mesopores with pore size < 3 nm, which contributed to its higher mesopore surface area, the larger MW NOM could hardly access such pores.

Figure 2 also demonstrates that even at the high PAC dosage of 500 mg/L, the residual NOM was still significant. To further understand the adsorbability of NOM by PAC, an extremely high carbon dose (2000 mg/L) was applied to investigate the adsorption properties of NOM on two PACs (Fig. 3).

Figure 3 shows that the adsorption capacities of PAC3 and PAC1 were similar at an extremely high carbon dose. Although the accessible mesopore amount of PAC3 was less, the extremely high carbon dose could provide sufficient available mesopores to adsorb the higher MW NOM. NOM with 300 Da < AMW < 3000 Da was completely adsorbed with an increase in carbon dose from 500 mg/L to 2000 mg/L. However, the NOM with 100 Da < AMW < 300 Da was barely adsorbed even at this high carbon dose. The majority of this NOM fraction was demonstrated to be hydrophilic and thus could hardly be adsorbed onto the hydrophobic surface of PACs. Meanwhile, the NOM with 10000 Da < AMW < 30000 Da was not adsorbed because the outer surface of carbon particles was preferably covered

by the relatively smaller NOM, and extremely large NOM was unable to enter any pore of PACs.

The residual DOC at different carbon doses is shown in Fig. 4. The removal of DOC by PAC3 was higher than that by PAC1 at low carbon doses. With the increase in carbon dose, the removal of DOC by PAC1 gradually exceeded that of PAC3. The removal of DOC by the two PACs was almost equal at an extremely high carbon dose. The changing trend of DOC with PAC dosage was similar to the results obtained through HPSEC. The DOC data can serve as corroboration for the results of HPSEC.

Therefore, in an emergency treatment of water pollution events, the selection of PAC should consider both the PSD of PAC and the MWD of NOM specifically. If the MWD of the NOM does not match the PSD of PACs, the adsorption sites of PACs could not be used efficiently.

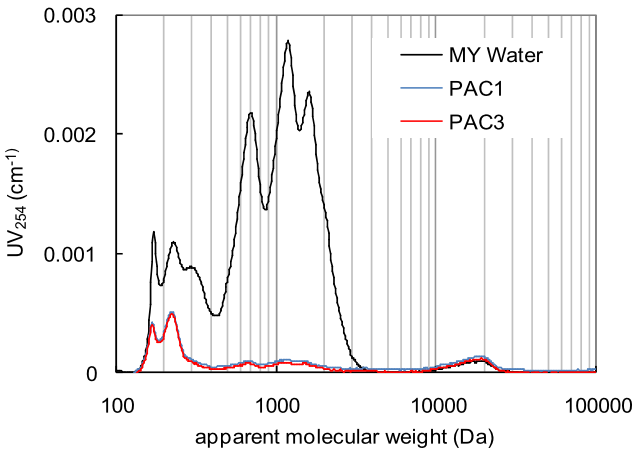

Fig. 3 AMW distribution of NOM for MY reservoir water before and after adsorption at a high PAC dosage

3.3 Comparison of Simultaneous and Preloaded Adsorption for MP

PAC2 and PAC1 were chosen for the adsorption tests of MP in OFW, MY water, and MPS water. The two PACs had similar mesopore size distribution and different mesopore surface area and volume. Two patterns of PAC adsorption for MP were conducted to mimic the PAC dosing before and after the chemical compound contamination spot. If PAC was dosed before the contamination spot, some of the adsorption sites of PAC would be initially occupied by NOM, referred to as preloaded adsorption. In the case of PAC dosing after the contamination point, NOM and target organic pollutants would be adsorbed simultaneously, referred to as simultaneous adsorption. One pattern of experiment was conducted using PAC2 and PAC1 pre-dosed into natural water to determine the effect of preloaded NOM on the adsorption of MP. In parallel, the other pattern of experiment was conducted using fresh PAC2 and PAC1 in natural water, indicating that MP and NOM were in contact with PAC simultaneously.

3.3.1 Adsorption isotherms

Figure 5 shows the adsorption isotherms of MP in OFW, MY, and MPS for fresh and preloaded PAC1 and PAC2, respectively. The adsorption capacity of PAC2 is higher than that of PAC1 for MP in OFW. The MW of MP was 263.5, and such small MW organics were primarily adsorbed by micropores. PAC2 has 1037 m^2/g of surface area in micropores, whereas PAC1 only has 780 m^2/g (Table 1). PAC2 could provide more available adsorption sites than PAC1 for MP. Therefore, the adsorption capacity of PAC2 was stronger than that of PAC1 in OFW.

Figure 5 also reveals that the adsorption capacities of MP in MY and MPS waters were significantly less than that in

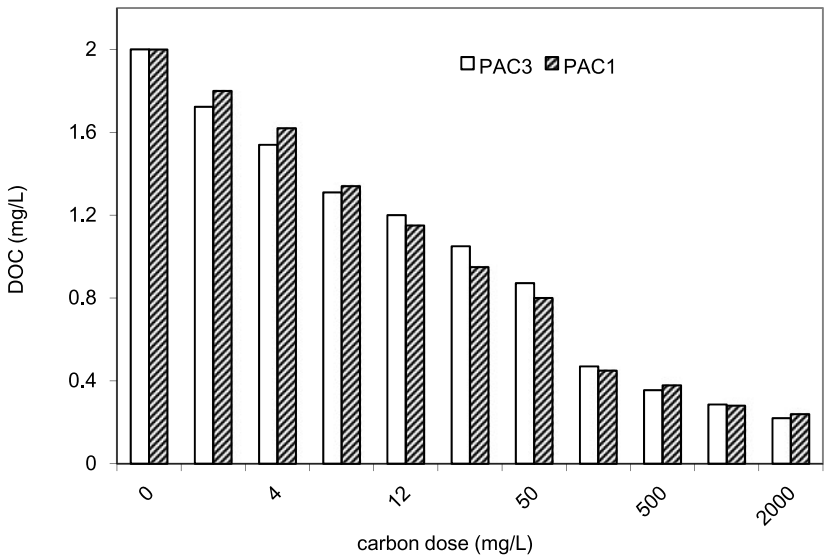

Fig. 4 DOC variation of the MY reservoir water before and after adsorption at different PAC dosages

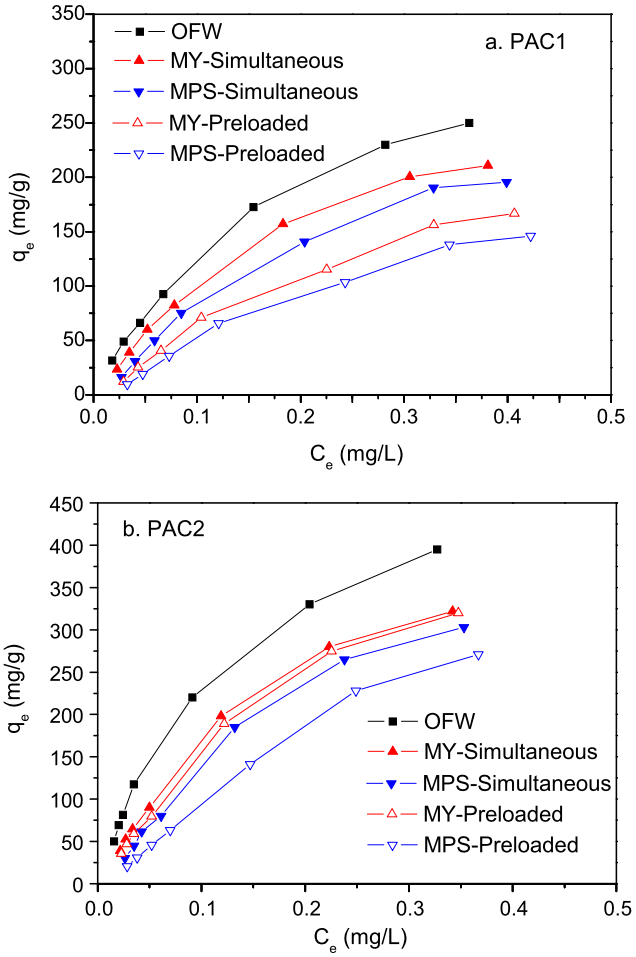

Fig. 5 Adsorption isotherms of MP on PACs in OFW and two natural waters (**a** PAC1; **b** PAC2)

OFW, indicating that NOM could compete for adsorption sites with MP on PACs. In addition, the adsorption capacity of MP by PAC1 in simultaneous adsorption was significantly higher than that in preloaded adsorption. During the preloading process, NOM could enter the pores or cover the outer surfaces of PAC preferentially, thus impeding the entry of MP into the pores when MP was spiked into the solution. Therefore, the removal efficiency of MP was reduced. Figure 5 also demonstrates that the adsorption capacity of MP in MY water was higher than that in MPS water both in simultaneous and preloaded adsorption. Table 2 presents the comparisons of the main MW fraction and the hydrophilic/hydrophobic property of NOM in MY and MPS waters. Compared with the NOM in MY water, the NOM in MPS water had a significantly higher NOM concentration, and more fractions of NOM in MPS were hydrophobic. In addition, NOM in MPS water contained slightly more MW fractions in the range of 500 Da < MW < 3000 Da. Thus, the NOM of MPS water could be easily adsorbed onto PAC, and consequently, more adsorption sites were taken by small NOM, and stronger pore blockage would be expected when PAC was preloaded in MPS water.

Figure 5 further reveals that preloading with NOM had no significant difference in the adsorption capacity of MP by PAC2 in MY water between simultaneous and preloaded adsorption. This finding could be explained by the relatively higher number of mesopores in PAC2. Not only were the mesopore surface area and volume of PAC2 higher than those of PAC1, PAC2 also provided more available mesopores with pore size > 3 nm.

Compared with MY water, MPS water contained more NOM fractions with higher MW. Although PAC2 can provide sufficient available mesopores to adsorb the higher MW NOM in MY water, pore blockage of PAC2 would occur when preloaded adsorption was conducted in MPS water, as shown in Fig. 5.

3.3.2 Adsorption kinetics

The effect of preloaded and simultaneous adsorption on the adsorption kinetics was investigated quantitatively using the kinetic parameter D_s. The diffusion rate of MP on PACs under the two patterns of adsorption can be reflected by the D_s value. The K and $1/n$ parameters in HSDM were obtained using the Freundlich model fitting, and D_s values were calculated by fitting the kinetic data into HSDM. Table 3 gives the values of K, $1/n$, and D_s for adsorption of MP onto PACs in OFW, simultaneous adsorption in MY, and MPS waters. The D_s values obtained for simultaneous adsorption in natural waters are close to those obtained in OFW. For PAC2, the D_s obtained in OFW, MY water, and MPS water were 1.0E−10, 0.97E−10, and 0.95E−10 cm^2/min, respectively, whereas for PAC1, the D_s were 0.67E−10, 0.65E−10, and 0.63E−10 cm^2/min, respectively. The relative intensity of direct adsorption site competition and the pore blockage effect determined how NOM affected the MP adsorption in simultaneous adsorption. When MP and NOM were in contact with PAC simultaneously, NOM cannot immediately block the PAC pores, and they compete with MP by direct competition for adsorption sites. The extent of diffusion of MP on PACs was not seriously affected by NOM in simultaneous adsorption. Therefore, the D_s values obtained in natural water were similar with that obtained in OFW. The data in Table 3 also indicated that the D_s values were independent of PAC doses when fresh PACs were used. With the increase in the PAC dose, only the removal of MP increased.

Table 4 lists the D_s values obtained by fitting the preloaded adsorption kinetic data of PAC2 and PAC1 in two natural waters using the pseudo-single solute HSDM. With the decrease in carbon dose, the D_s values corresponding to PAC1 decreased significantly, indicating that the NOM pore blockage effect was the primary competitive mechanism in preloaded adsorption. As shown in Table 4, with similar carbon doses of PAC1, the preloaded D_s values were lower than

Table 3 HSDM parameters for simultaneous adsorption of PAC1 and PAC2 in OFW, MY and MPS waters

	Dose (mg/L)	PAC1			PAC2		
		K (mg/g)(L/mg)$^{1/n}$	D_s (cm^2/min)	$1/n$	K (mg/g)(L/mg)$^{1/n}$	D_s (cm^2/min)	$1/n$
OFW	5	14.59	0.67 E−10	0.7	17.74	1.00 E−10	0.7
	10	14.59	0.67 E−10	0.7	17.74	1.00 E−10	0.7
MY	5	12.53	0.65 E−10	0.7	14.59	0.97 E−10	0.7
	10	12.53	0.65 E−10	0.7	14.59	0.97 E−10	0.7
MPS	5	6.35	0.63 E−10	0.7	9.12	0.95 E−10	0.7
	10	6.35	0.63 E−10	0.7	9.12	0.95 E−10	0.7

Table 4 HSDM parameters for preloaded adsorption of PAC2 and PAC1 in MY and MPS waters

	Dose (mg/L)	PAC1			PAC2		
		K (mg/g)(L/mg)$^{1/n}$	D_s (cm^2/min)	$1/n$	K (mg/g)(L/mg)$^{1/n}$	D_s (cm^2/min)	$1/n$
MY	2	16.44	2.00 E−12	0.7	25.07	0.97 E−10	0.7
	5	11.80	4.47 E−12	0.7	17.29	0.97 E−10	0.7
	10	11.04	7.59 E−12	0.7	14.07	0.97 E−10	0.7
	20	7.29	2.00 E−11	0.7	8.63	0.97 E−10	0.7
	50	4.13	5.25 E−11	0.7	4.36	0.97 E−10	0.7
MPS	2	5.02	1.83 E−12	0.7	8.09	3.10 E−12	0.7
	5	4.89	2.92 E−12	0.7	7.43	7.24 E−12	0.7
	10	4.58	4.93 E−12	0.7	7.25	9.42 E−12	0.7
	20	4.32	1.00 E−11	0.7	5.03	3.72 E−11	0.7
	50	3.24	1.74 E−11	0.7	3.45	6.03 E−11	0.7

the simultaneous D_s values shown in Table 3 due to the pore blockage in preloaded adsorption. Meanwhile, a comparison of D_s values corresponding to PAC2 shows that only a slight pore blockage effect of NOM was found in MY water.

In addition, the D_s values relating to preloaded adsorption for both PACs were significantly lower than those relating to simultaneous adsorption with the same carbon dosage in MPS water, indicating that the pore blockage effect of NOM occurred for both PAC2 and PAC1. Table 4 also reveals that the D_s of MP for the two PACs decreased with decreasing carbon dose. A lower carbon dose resulted in a higher surface concentration of NOM on PAC. Thus, the pore blockage effect became more severe. Therefore, when MP was spiked into the solution, it would hardly be able to enter the pores of PACs. Li et al. also found that the diffusion rate of trace level atrazine onto PACs could be significantly reduced due to the pore blockage effect of NOM (Li et al. 2003c).

Figure 6 presents the relationship between NOM surface load and D_s values. Higher surface concentration of NOM resulted in a lower D_s value. Additionally, the effect of pore blockage by NOM was more pronounced for PAC1 than for PAC2. This finding could be explained by the larger amount of available mesopores (pore size > 3 nm) of PAC2. The

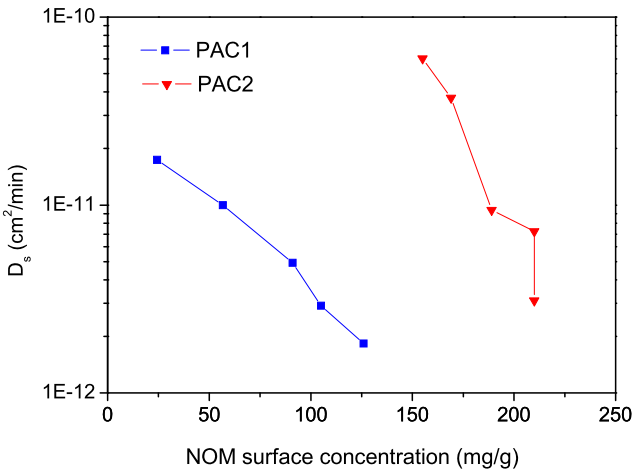

Fig. 6 D_s changes with the surface load of NOM on PACs

NOM surface coverage rate on PAC2 was lower than that on PAC1 with the same surface concentration of NOM due to the larger number of mesopores in PAC2. Therefore, the diffusion rate of MP on PAC2 was higher than that on PAC1 when MP was spiked into the solution. Hence, the D_s of MP for PAC2 was higher than that for PAC1 with the same surface concentration of NOM, as shown in Fig. 6.

With the same carbon dose, the D_s values in preloaded adsorption were lower than the simultaneous D_s. This fact implies that in the process of water treatment with PAC, the removal efficiency would be significantly affected by the selection of PAC dosing patterns. The dosing points should not be placed in front of the pollution point to avoid the negative effect of pore blockage.

4 Concluding remarks

In the event of source water pollution by agricultural chemicals, the selection of PAC should be based on the suitability between the MWD of NOM and the PSD of PAC. The adsorption of the NOM fraction with MW lower than 500 Da by PAC was primarily determined by the micropore surface area, and the adsorption of that with 500 Da $<$ MW $<$ 3000 Da was primarily affected by both mesopore surface area and mesopore size distribution. The PAC mesopore surface area with pore size $>$ 3 nm was a critical property that had great effect on the adsorption of the NOM fraction in this molecular weight range.

NOM could compete with target organic compounds on PAC through two major mechanisms, namely, direct competition for surface sites and pore blockage. Competition for sites had a negative effect on the adsorption of target organic compounds in simultaneous adsorption, whereas the effect of pore blockage was significantly more pronounced in preloaded adsorption.

The D_s value, generally used to evaluate the adsorption kinetics, could be an index reflecting the extent of the pore blockage effect, which was determined by the adsorption pattern, the PSD of PAC, and the MWD of NOM. The D_s values of MP onto PACs were almost similar for simultaneous adsorption in OFW and natural waters, and were independent of carbon dose. However, the removal of MP increased with increasing PAC dose. For preloaded adsorption, the D_s values decreased with decreasing carbon dose or increasing NOM surface concentration.

Acknowledgements The current work was financially supported by the National Natural Science Foundation of China (Grant No. 50878204) and National 863 Research and Development Program of China (2008AA06A414).

References

Abou-Mesalam, M.M.: Sorption kinetics of copper, zinc, cadmium and nickel ions on synthesized silico-antimonate ion exchanger. Colloids Surf. A, Physicochem. Eng. Asp. **225**(1–3), 85–94 (2003)

Akhtar, M., Iqbal, S., Bhanger, M.I., Zia-Ul-Haq, M., Moazzam, M.: Sorption of organophosphorous pesticides onto chickpea husk from aqueous solutions. Colloids Surf. B, Biointerfaces **69**(1), 63–70 (2009)

Arduini, F., Ricci, F., Tuta, C.S., Moscone, D., Amine, A., Palleschi, G.: Detection of carbamic and organophosphorous pesticides in water samples using a cholinesterase biosensor based on Prussian Blue-modified screen-printed electrode. Anal. Chim. Acta **580**(2), 155–162 (2006)

Carter, M.C., Weber, W.J.: Modeling adsorption of Tce by activated carbon preloaded by background organic-matter. Environ. Sci. Technol. **28**(4), 614–623 (1994)

De Souza, D., Machado, S.A.S.: Study of the electrochemical behavior and sensitive detection of pesticides using microelectrodes allied to square-wave voltammetry. Electroanalysis **18**(9), 862–872 (2006)

Ding, L., Marinas, B.J., Schideman, L.C., Snoeyink, V.L.: Competitive effects of natural organic matter: parametrization and verification of the three-component adsorption model COMPSORB. Environ. Sci. Technol. **40**(1), 350–356 (2006)

Gogate, P.R., Shriwas, A.K.: Ultrasonic degradation of methyl parathion in aqueous solutions: intensification using additives and scale up aspects. Sep. Purif. Technol. **79**(1), 1–7 (2011)

Hand, D.W., Crittenden, J.C., Thacker, W.E.: User-oriented batch reactor solutions to the homogeneous surface-diffusion model. J. Environ. Eng. **109**(1), 82–101 (1983)

He, Q., Peng, S.J., Zhai, J., Xiao, H.W.: Development and application of a water pollution emergency response system for the Three Gorges Reservoir in the Yangtze River, China. J. Environ. Sci. **23**(4), 595–600 (2011)

Hung, H.W., Lin, T.F., Baus, C., Sacher, F., Brauch, H.J.: Competitive and hindering effects of natural organic matter on the adsorption of MTBE onto activated carbons and zeolites. Environ. Technol. **26**(12), 1371–1382 (2005)

Kilduff, J.E., Karanfil, T., Weber, W.J.: Competitive effects of nondisplaceable organic compounds on trichloroethylene uptake by activated carbon. I. Thermodynamic predictions and model sensitivity analyses. J. Colloid Interface Sci. **205**(2), 271–279 (1998)

Li, B.X., He, Y.Z., Xu, C.L.: Simultaneous determination of three organophosphorus pesticides residues in vegetables using continuous-flow chemiluminescence with artificial neural network calibration. Talanta **72**(1), 223–230 (2007)

Li, C.Y., Wang, Z.G., Zhan, G.Q.: Electrochemical investigation of methyl parathion at gold-sodium dodecylbenzene sulfonate nanoparticles modified glassy carbon electrode. Colloids Surf. B, Biointerfaces **82**(1), 40–45 (2011)

Li, Q.L., Marinas, B.J., Snoeyink, V.L., Campos, C.: Three-component competitive adsorption model for flow-through PAC systems. 1. Model development and verification with a PAC/membrane system. Environ. Sci. Technol. **37**(13), 2997–3004 (2003a)

Li, Q.L., Snoeyink, V.L., Mariaas, B.J., Campos, C.: Elucidating competitive adsorption mechanisms of atrazine and NOM using model compounds. Water Res. **37**(4), 773–784 (2003b)

Li, Q.L., Snoeyink, V.L., Marinas, B.J., Campos, C.: Pore blockage effect of NOM on atrazine adsorption kinetics of PAC: the roles of PAC pore size distribution and NOM molecular weight. Water Res. **37**(20), 4863–4872 (2003c)

McKay, G., Choy, K.K.H.: Sorption of cadmium, copper, and zinc ions onto bone char using crank diffusion model. Chemosphere **60**(8), 1141–1150 (2005)

Schwarzenbach, R.P., Gschwend, P.M., Imboden, D.M.: Environmental Organic Chemistry, 2nd edn. Wiley, Hoboken (2003)

Shin, E.W., Rowell, R.M.: Cadmium ion sorption onto lignocellulosic biosorbent modified by sulfonation: the origin of sorption capacity improvement. Chemosphere **60**(8), 1054–1061 (2005)

Wei, Q.S., Wang, D.S., Wei, Q., Qiao, C.G., Shi, B.Y., Tang, H.X.: Size and resin fractionations of dissolved organic matter and trihalomethane precursors from four typical source waters in China. Environ. Monit. Assess. **141**(1–3), 347–357 (2008)

Zhang, B., Qin, Y., Huang, M.X., Sun, Q., Li, S., Wang, L.Q., Yu, C.H.: SD-GIS-based temporal-spatial simulation of water quality in sudden water pollution accidents. Comput. Geosci. **37**(7), 874–882 (2011)